

Ozone Formation in Laser Flash Photolysis of Oxoacids and Oxoanions of Chlorine and Bromine†

BY ULRIK K. KLÄNING*

Department of Chemistry, University of Aarhus, Langelandsgade 140,
DK-8000 Aarhus C, Denmark

AND KNUD SEHESTED

Accelerator Department, Risø National Laboratory, DK-4000 Roskilde, Denmark

AND THOMAS WOLFF

University of Siegen, D-5900 Siegen 21, Federal Republic of Germany

Received 11th January, 1984

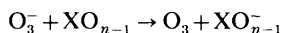
The kinetics of ozone formation in the photolysis of oxygen-containing solutions of HClO, ClO⁻, ClO₂⁻, ClO₃⁻, HBrO, BrO⁻ and BrO₃⁻ has been studied by laser flash photolysis and conventional flash photolysis. The usual assumption, that ozone only forms in the reaction of oxygen atoms in the spin-triplet ground state with molecular oxygen:



subsequent to the primary process



is found to be valid for solutions at pH ≤ 10 but not for more strongly alkaline solutions. The rate constants of the reactions of O with O₂ and BrO₃⁻ are found to be 4.0 × 10⁹ and 1.5 × 10⁷ dm³ mol⁻¹ s⁻¹, respectively. The formation of ozone in strongly alkaline solutions can be accounted for by the additional processes



with rate constants in the range 5 × 10⁸ to 1.5 × 10⁹ dm³ mol⁻¹ s⁻¹ subsequent to



and the primary process



Previous investigations¹⁻⁴ have shown that ozone is a product in the photolysis of oxygen-containing aqueous solutions of the oxoanions ClO⁻, ClO₃⁻, BrO⁻, BrO₂⁻, BrO₃⁻ and IO₄⁻. The formation of ozone has been assumed to take place in the reaction of oxygen atoms in the spin-triplet ground state with molecular oxygen



subsequent to the primary photochemical process in which O is formed:



† Presented in part at the 11th International Conference on Photochemistry, Maryland, U.S.A.

The ozone produced can be identified in flash-photolytic experiments by its strong absorption band centred at 260 nm ($\epsilon_{260} = 3300 \text{ dm}^3 \text{ mol}^{-1} \text{ cm}^{-1}$)⁵ and by its decay kinetics in alkaline solution.^{3, 6}

To verify the mechanism of ozone formation we have measured the kinetics of absorbance change in the region $240 < \lambda/\text{nm} < 600$ with a time resolution of 10^{-8} s in laser flash photolysis of acid, neutral and alkaline O_2 -free and O_2 -containing solutions of HClO , ClO^- , ClO_2^- , ClO_3^- , HBrO , BrO^- and BrO_3^- .

The laser-flash-photolysis experiments were supplemented with conventional flash photolysis and pulse-radiolysis measurements of alkaline solutions of BrO_3^- .

EXPERIMENTAL

The apparatus for laser flash photolysis was as described previously⁷ except for interchange in the laser flash photolysis apparatus of glass lenses with quartz lenses and of the RCA 1P28 photomultiplier with a RCA 4840 photomultiplier. The 193, 248.5 and 308 nm emissions of the Lambda Physik EMG 500 excimer laser were collimated in a 2 cm wide beam into the 2 cm long and 0.3 cm wide rectangular quartz cell perpendicular to the monitoring light.

Owing to absorption of laser light in the solution, the concentration of photoproducts decreases with the distance from the entrance window of the laser beam. The concentration of the solute was adjusted to an absorption of laser light in the cell of $< 90\%$. In most experiments the absorption was $< 50\%$. Calculations⁸ show that the effect of absorption of laser light in the cell on the measured kinetics of a second-order reaction is negligible for an absorption of laser light $< 50\%$. At 90% absorption the calculations show that measured rate constants for second-order reactions are 10–20% higher than those measured for solutions with uniform concentration of reactants.

The light intensity of the pulsed monitoring light was sufficiently constant for measurements up to 2×10^{-4} s after the laser flash. To reduce photolysis by the monitoring light, 'cut off' filters were used. The solutions were saturated with O_2 or air by bubbling N_2 through the solution for 3 min. No effect on the experimental results could be detected by prolonged bubbling.

Spectra were measured point-by-point, changing the monochromator setting after the flash. The solutions were replaced after each flash. Attenuation ($8 \times$) of the 100–200 mJ flash showed proportionality between absorbance change and laser light intensity. Thus no effects of multiphoton absorption or of secondary photolysis of photoproducts were detected.

ClO_3^- and BrO_3^- solutions with $[\text{BrO}_3^-] < 10^{-3} \text{ mol dm}^{-3}$ were irradiated with laser light of wavelength 193 nm; BrO_3^- solutions with $0.025 < [\text{BrO}_3^-]/\text{mol dm}^{-3} < 0.1$ and solutions of ClO_2^- , HClO and HBrO with 248.5 nm and solutions of ClO^- and BrO^- with 308 nm laser light.

Water used for the preparation of solutions for the pulse-radiolysis experiments was purified as described elsewhere.⁹ Water used in the photochemical experiments was deionized and distilled twice in an all-quartz apparatus. Gases were N_2 99.999% and O_2 99.995%. KClO_3 and KBrO_3 were Merck p.a., NaClO_2 was Matheson, Coleman and Bell analytical grade dried over P_2O_5 , assay 99% (iodometrically determined). $\text{NaClO} \cdot 5\text{H}_2\text{O}$, and $\text{NaBrO} \cdot 5\text{H}_2\text{O}$ were prepared as described,¹⁰ recrystallized from 2% aqueous NaOH solution and stored at -70°C . Solutions of $\text{NaBrO} \cdot 5\text{H}_2\text{O}$ and of $\text{NaClO} \cdot 5\text{H}_2\text{O}$ were analysed as follows. The concentration of hypohalite was determined by potentiometric titration with As^{III} in alkaline solution. The sum of the concentrations of hypohalite and halide was determined by potentiometric titration with Ag^+ of solutions in which hypohalite had been reduced with As^{III} . The analysis showed a content of halide in hypohalite of 1–2%, a content which did not have any effect on the results. The content of BrO_2^- and BrO_3^- in hypobromite determined iodometrically as BrO_3^- was $< 0.5\%$. BrO^- solutions were freed from Br^- by acidifying the solution and removing the Br_2 formed by bubbling N_2 through the solution for 10 min.

Pulse radiolysis and conventional flash photolysis were carried out as described previously.⁴ Computations were made as described elsewhere.⁴ All measurements were made at ambient temperature ($21 \pm 2^\circ\text{C}$).

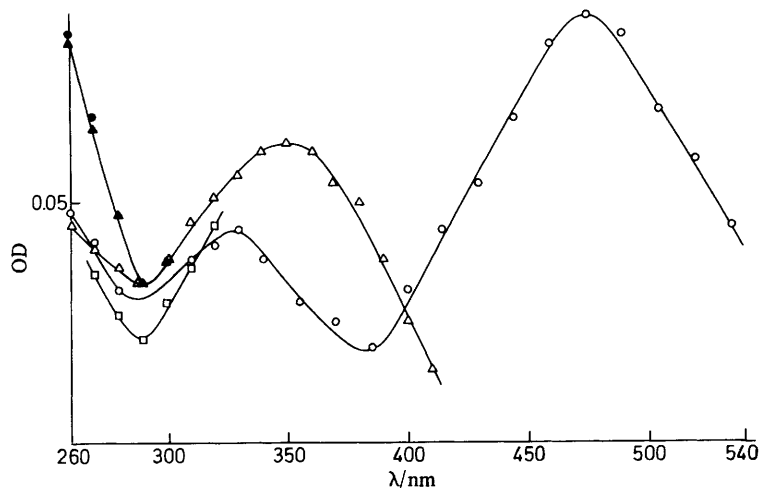
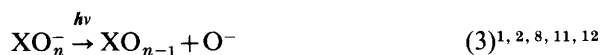


Fig. 1. Transient absorbance, OD, plotted against wavelength, λ/nm , recorded $2\ \mu\text{s}$ after laser flash irradiation (193 nm) of solutions containing (\circ and \bullet) $10^{-3}\ \text{mol dm}^{-3}$ KBrO_3 and (\triangle , \square and \blacktriangle) $10^{-3}\ \text{mol dm}^{-3}$ KClO_3 . Open symbols, O_2 -free solutions; solid symbols, $[\text{O}_2] = 1.27 \times 10^{-3}\ \text{mol dm}^{-3}$. All solutions neutral except for \square , $[\text{HClO}_4] = 2 \times 10^{-3}\ \text{mol dm}^{-3}$.

RESULTS AND DISCUSSION

O_2 -FREE SOLUTIONS

The primary process (2) cannot be observed by photolysis of O_2 -free solutions. The absorbance changes are assigned to the primary processes



and to secondary processes in agreement with previous results. Transient absorption bands centred at 350 nm in solutions of ClO_3^- and at 475 nm in solutions of BrO_3^- were observed (fig. 1). These bands were assigned to ClO_2 and BrO_2 [reaction (3)], respectively, in accordance with previous studies.^{2, 12}

A band centred at 330 nm in BrO_3^- solutions is assigned to BrO^- formed in the primary process (5). Similarly, the observation that the transient absorbance at $270 < \lambda/\text{nm} < 330$ in ClO_3^- solutions after flash excitation is smaller in acid than in neutral solution is ascribed to the difference in absorbance of HClO and ClO^- formed in the primary process (5).²

A transient absorption band centred at 280 nm observed in flash-irradiated ClO_2^- solutions is assigned to formation of ClO^{14} in the primary process (3). The band decays

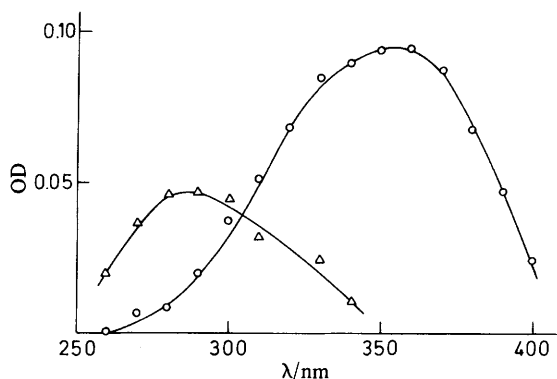
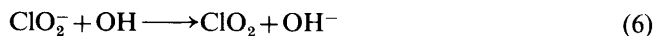
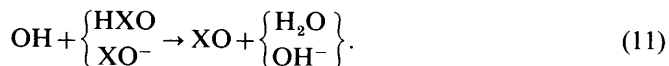
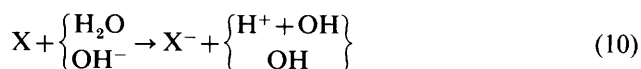


Fig. 2. Transient absorbance, OD, plotted against wavelength, λ/nm , recorded (Δ) *ca.* 10^{-2} μs and (\circ) $4 \mu\text{s}$ after laser flash irradiation (248.5 nm) of a solution containing 1.65×10^{-3} mol dm^{-3} NaClO_2 .

into a band centred at 360 nm (fig. 2) which we ascribe to ClO_2 formed in the reactions¹⁵



The transient absorption bands at 310 and 280 nm observed by laser flash photolysis of hypochlorite solutions at $\text{pH} < 10$ are assigned to halogen atoms,¹⁶ formed in reactions (3) and (4). These bands, which are thought to be due to charge transfer from solvent,¹⁶ decay into two new bands centred at 280 and 340 nm (fig. 3), which we assign to ClO^1 and BrO^{17} formed in the reactions⁸



In strongly alkaline solutions of ClO^- and BrO^- , the absorption bands of Cl and Br are not observed owing to the fast reaction (10).⁸

O_2 -CONTAINING SOLUTIONS ($\text{pH} < 10$)

The increase in absorbance by addition of O_2 , ΔOD , observed at $\lambda < 300$ nm after laser irradiation is ascribed to the formation of ozone. The yield and kinetics of the formation of O_3 depend on pH . At $\text{pH} < 10$, O_3 is formed in O_2 -containing HClO , ClO_3^- and BrO_3^- solutions in a first-order process. ΔOD measured at $240 < \lambda/\text{nm} < 300$ increases with time to a limiting value ΔOD_∞ . Fig. 3(a) shows that ΔOD_∞ of a solution of HClO plotted against wavelength fits the absorption spectrum of O_3 .⁵ We assign the formation of O_3 to the reaction (1) subsequent to the primary process (2). Fig. 4 shows a plot of $\ln(\Delta\text{OD}_\infty - \Delta\text{OD})$ measured at 260 nm against

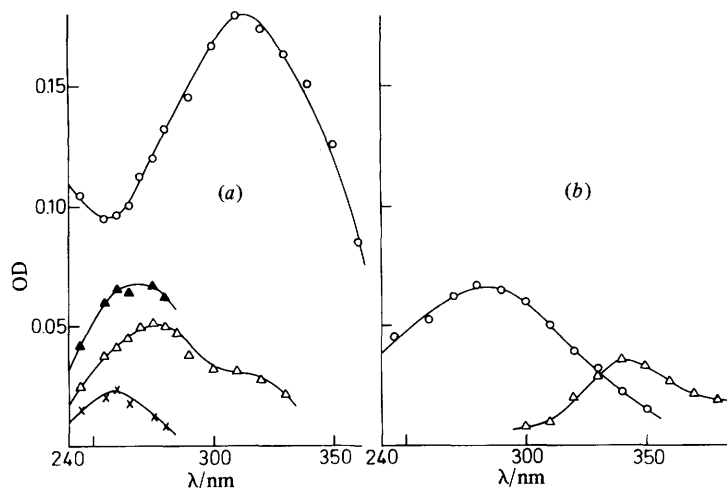


Fig. 3. Transient absorbance, OD, plotted against wavelength, λ/nm , after laser flash irradiation (308 nm) of a solution containing (a) $4.85 \times 10^{-3} \text{ mol dm}^{-3} \text{ HClO}$ and $2.5 \times 10^{-2} \text{ mol dm}^{-3} \text{ HClO}_3$ and (b) $1.53 \times 10^{-3} \text{ mol dm}^{-3} \text{ HBrO}$ and $10^{-3} \text{ mol dm}^{-3} \text{ HClO}_4$. \circ , Recorded *ca.* $10^{-2} \mu\text{s}$ after flash; \triangle and \blacktriangle , recorded $1 \mu\text{s}$ after flash. Open symbols, O_2 -free solutions; solid symbols, $[\text{O}_2] = 1.27 \times 10^{-3} \text{ mol dm}^{-3}$; \times , ΔOD_∞ (difference between OD of O_2 -containing and O_2 -free solutions).

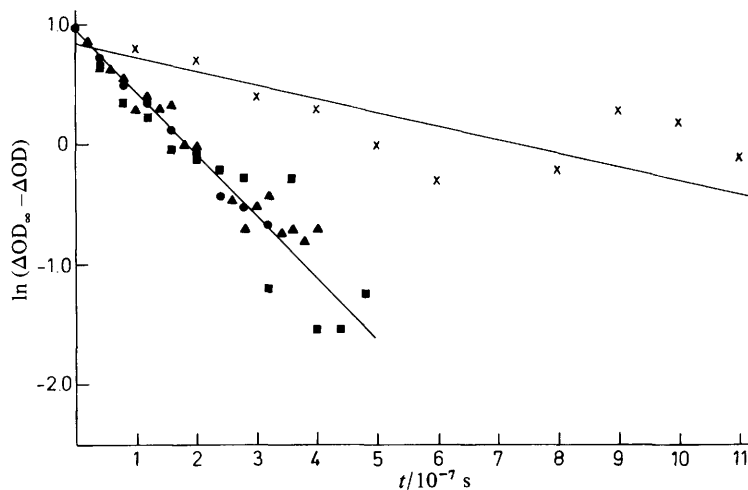


Fig. 4. First-order plot of increase of absorbance at 260 nm in O_2 -containing solutions after laser flash irradiation. \times and \bullet , $[\text{BrO}_3^-] = 5 \times 10^{-4} \text{ mol dm}^{-3}$ (\times , $[\text{O}_2] = 2.54 \times 10^{-4}$; \bullet , $[\text{O}_2] = 1.27 \times 10^{-3} \text{ mol dm}^{-3}$), laser light 193 nm. \blacksquare , $[\text{ClO}_3^-] = 10^{-3} \text{ mol dm}^{-3}$, $[\text{O}_2] = 2.54 \times 10^{-3} \text{ mol dm}^{-3}$, laser light 193 nm; \blacktriangle , $[\text{HClO}] = 4.85 \times 10^{-3} \text{ mol dm}^{-3}$, $[\text{O}_2] = 2.54 \times 10^{-3} \text{ mol dm}^{-3}$, laser light 308 nm.

time in O_2 -saturated solutions of $4.85 \times 10^{-3} \text{ mol dm}^{-3} \text{ HClO}$, $1.0 \times 10^{-3} \text{ mol dm}^{-3} \text{ ClO}_3^-$ and $5.0 \times 10^{-4} \text{ mol dm}^{-3} \text{ BrO}_3^-$ and in air-saturated solutions of $5.0 \times 10^{-4} \text{ mol dm}^{-3} \text{ BrO}_3^-$. From the slopes of the straight lines in fig. 4, which are proportional to $[\text{O}_2]$, we find, by taking $[\text{O}_2] = 1.27 \times 10^{-3} \text{ mol dm}^{-3}$ in O_2 -saturated solutions¹⁸ and $2.54 \times 10^{-4} \text{ mol dm}^{-3}$ in air-saturated solutions,

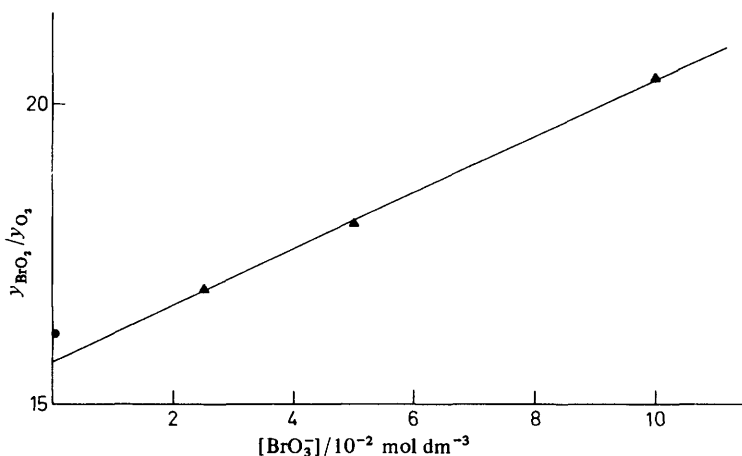


Fig. 5. Yield of BrO_2 relative to yield of O_3 , $y_{\text{BrO}_2}/y_{\text{O}_3}$, in laser-flash-irradiated BrO_3^- solutions plotted against $[\text{BrO}_3^-]$ (laser light: ●, 193; ▲, 248.5 nm).

$k_1 = 4.0 \times 10^9 \text{ dm}^3 \text{ mol}^{-1} \text{ s}^{-1}$. The fact that the slopes in fig. 4 are proportional to $[\text{O}_2]$ indicates that the reactions of oxygen atom with the solutes HClO , ClO_3^- and BrO_3^- are slow compared with the reaction of oxygen atom with molecular oxygen.

By photolysis of solutions containing $0.025 < [\text{BrO}_3^-]/\text{mol dm}^{-3} < 0.1$ with laser light of wavelength 248.5 nm we were able to detect a reaction which we assume is



Assuming that O_3 and BrO_2 are formed by reactions (1) and (3) only their relative yields $y_{\text{BrO}_2}/y_{\text{O}_3}$ may be expressed by

$$y_{\text{BrO}_2}/y_{\text{O}_3} = A(k_1[\text{O}_2] + k_{12}[\text{BrO}_3^-])/(k_1[\text{O}_2]) \quad (13)$$

where

$$A = \lim_{[\text{BrO}_3^-] \rightarrow 0} y_{\text{BrO}_2}/y_{\text{O}_3}$$

is the branching ratio for the photochemical processes (3) and (2). We find $k_{12}/k_1 = 3.8 \times 10^{-3}$ from a plot (fig. 5) of the ratio $y_{\text{BrO}_2}/y_{\text{O}_3}$ against $[\text{BrO}_3^-]$. Values of $y_{\text{BrO}_2}/y_{\text{O}_3}$ were obtained from

$$y_{\text{BrO}_2}/y_{\text{O}_3} = \Delta\text{OD}^{475} \times (\epsilon_{\text{O}_3}^{260} + \epsilon_{\text{BrO}_2^-}^{260}) / (\epsilon_{\text{BrO}_2^-}^{475} \times \Delta\text{OD}_{\infty}^{260}). \quad (14)$$

ΔOD^{475} is the absorbance at 475 nm measured just after the flash irradiation and $\epsilon_{\text{BrO}_2^-}^{475}$, $\epsilon_{\text{BrO}_2^-}^{260}$ and $\epsilon_{\text{O}_3}^{260}$ are the corresponding extinction coefficients of BrO_2 , BrO_2^- and O_3 at the given wavelengths.^{5, 17, 19}

The fact that no reaction with water is observed is in keeping with the assignment of the ozone precursor to an oxygen atom in a spin-triplet state since the route to H_2O_2 is forbidden because it involves a change of spin multiplicity and the route to 2OH is not feasible thermodynamically.²⁰ The reason for the relative sluggishness of the reactions with the solutes HClO , ClO_3^- and BrO_3^- might be that the pathway to products in these reactions also involves a spin-forbidden step (e.g. with the intermediate formation of peroxy compounds).

Table 1 shows yields of ozone relative to yields of the products formed in the primary process (3). The yields were obtained from measured absorbance by using

Table 1. Ratio of yields at pH < 10, $y_{O_3}/y_{XO_{n-1}}$, and at pH > 12, $Y_{O_3}/Y_{XO_{n-1}}$

species	$y_{O_3}/y_{XO_{n-1}}$	$Y_{O_3}/Y_{XO_{n-1}}$
HClO	0.2 ^a	—
ClO ⁻	0.08 ^a	0.3 ^a
HBrO	< 0.01	—
BrO ⁻	< 0.01 ^b	0.3, ^b 0.4 ^c
ClO ₂ ⁻	< 0.01	< 0.01
ClO ₃ ⁻	0.1	—
BrO ₃ ⁻	0.062, ^a 0.064 ^e	0.5, ^f 0.6 ^c

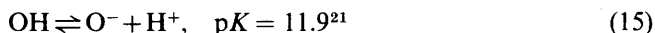
^a Calculated from Y_{ClO} by taking $Y_{ClO} = 2Y_{Cl}$; ^b calculated from Y_{BrO} by taking $Y_{BrO} = 2Y_{Br}$; ^c calculated from values in ref. (3) (see text); ^d laser flash wavelength 193 nm; ^e laser flash wavelength 248.5 nm, determined by extrapolation to $[BrO_3^-] = 0$ (fig. 5); ^f conventional flash photolysis.

equations analogous to eqn (14). Note that $y_{O_3}/y_{XO_{n-1}} \ll 1$ for all solutes in accordance with the view that process (2) is a spin-forbidden process. Further, note that the branching ratio, y_{O_3}/y_{BrO_2} , between processes (2) and (3) appears to be the same for photolysis with light of wavelengths 193 and 248.5 nm.

O₂-CONTAINING SOLUTIONS (pH > 12)

On photolysis of O₂-containing solutions of ClO⁻, BrO⁻ and BrO₃⁻ at pH > 12 we observe the formation of O₃ with a much higher yield and at a much slower rate than observed in solutions at pH < 10.

On photolysis of O₂-containing solutions of ClO⁻, ClO₂⁻, BrO⁻ and BrO₃⁻ at pH > 12, O₃⁻ is observed in addition to species observed at pH < 10. O₃⁻ is formed in alkaline solution by the reactions



subsequent to the primary reaction (3). O₃⁻ is not observed at pH < 10 owing to fast reactions of OH: $[2OH \rightarrow H_2O_2]$, reactions (6) and (11)].

The following observations indicate that most of the ozone formed at pH > 12 is produced in reactions of O₃⁻ with primary or secondary formed halogen oxides. Fig. 6 shows transient spectra measured 0.5 and 45 μs after laser flash irradiation of BrO₃⁻ solutions at pH 13, saturated with O₂ or rendered O₂-free before irradiation. The difference in absorbance at $240 < \lambda/nm < 280$ between O₂-saturated and O₂-free solutions 0.5 μs after the flash is assigned to the formation of O₃ in reaction (1) subsequent to the primary process (2), in agreement with the assignment at pH < 10. In O₂-free solutions an additional band at 470 nm due to BrO₂ is observed. The unsymmetrical band at $\lambda \approx 450$ nm seen in O₂-saturated solutions is ascribed to a composite of the band at 470 nm due to BrO₂ and the band at 430 nm due to O₃⁻.²²

The difference in absorbance at $240 < \lambda/nm < 280$ between O₂-saturated and O₂-free solutions increases with time simultaneously with a decrease in absorbance at $350 < \lambda/nm < 550$. The rate of relative decrease of absorbance at 375 nm (O₃⁻) equals the rate of relative increase of absorbance at 260 nm (O₃) (fig. 7).

45 μs after the flash the absorption band at 470 nm has disappeared and the

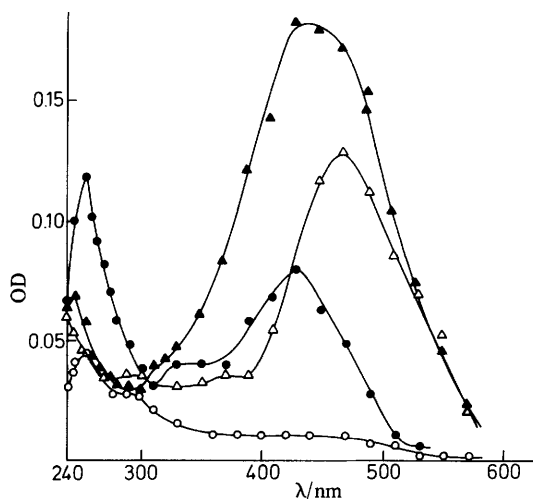


Fig. 6. Transient absorbance, OD, plotted against wavelength, λ/nm , after laser flash irradiation (248.5 nm) of solutions containing $0.05 \text{ mol dm}^{-3} \text{ KBrO}_3$ and $0.1 \text{ mol dm}^{-3} \text{ NaOH}$. Open symbols represent O_2 -free solutions; solid symbols, $[\text{O}_2] = 1.27 \times 10^{-3} \text{ mol dm}^{-3}$. \triangle and \blacktriangle , recorded $0.5 \mu\text{s}$ after flash; \circ and \bullet , recorded $45 \mu\text{s}$ after flash.

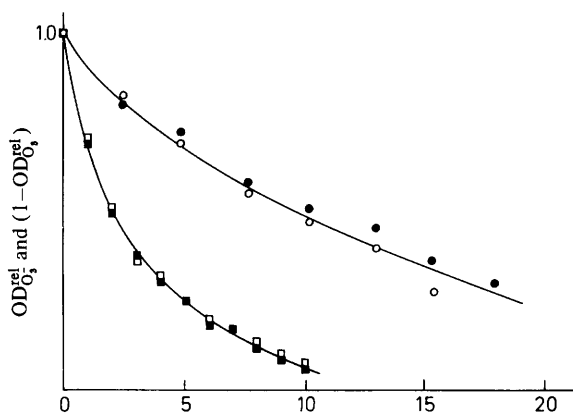


Fig. 7. Relative change in absorbance, $\text{OD}_{\text{O}_3}^{\text{rel}}$ and $1 - \text{OD}_{\text{O}_3}^{\text{rel}}$ calculated as $(\text{OD} - \text{OD}_{\infty}) / (\text{OD}_0 - \text{OD}_{\infty})$, plotted against time. \square and \blacksquare , $5 \times 10^{-2} \text{ mol dm}^{-3} \text{ BrO}_3^-$, $0.1 \text{ mol dm}^{-3} \text{ NaOH}$, laser light 248.5 nm; \circ and \bullet , $0.1 \text{ mol dm}^{-3} \text{ BrO}_3^-$, $0.1 \text{ mol dm}^{-3} \text{ NaOH}$, pulse radiolysis, 30 Gy per pulse. Open symbols, measured at 260 nm; closed symbols, measured at 375 nm. \circ and \bullet , $[\text{O}_2] = 2.5 \times 10^{-4} \text{ mol dm}^{-3}$; \square and \blacksquare , $[\text{O}_2] = 1.27 \times 10^{-3} \text{ mol dm}^{-3}$.

spectrum in the O_2 -saturated solution now contains an absorption band at 260 nm due to O_3 and one at 430 nm due to remaining O_3^- (fig. 6). After the disappearance of BrO_2 no further changes in $[\text{O}_3]$ and $[\text{O}_3^-]$ were detected in the next $150 \mu\text{s}$, which is in agreement with the rates of decay of $\text{O}_3^{\cdot-}$ and of $\text{O}_3^{\cdot-22}$ measured in solutions at the same pH and O_2 concentration. The small band at 260 nm observed after $45 \mu\text{s}$ in solutions which were freed of O_2 before the flash irradiation is probably due to O_3 , formed from traces of O_2 produced in primary process (5).

These observations suggest that O_3 is formed by a reaction of O_3^- with BrO_2 . Formation of ozone by pulse radiolysis of alkaline air-saturated BrO_3^- solutions corroborates this suggestion. In such experiments O_3^- and BrO_2 are formed from the primary radiolytical species O^- and e_{aq}^- , O_3^- by reaction (16) and BrO_2 by the reaction

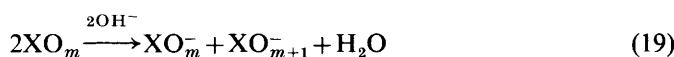


In the present experiments $[BrO_3^-]$ and $[O_2]$ were chosen to avoid formation of O_2^{2-} ,²³ and thus it was possible to assign the increase of absorbance observed at $\lambda < 300$ nm to the formation of ozone. The kinetics of the formation of ozone was similar to that observed in laser flash photolysis. The formation took place simultaneously with a decrease in the absorbance of O_3^- and BrO_2 , and the rate of formation of O_3 was equal to the rate of disappearance of O_3^- (fig. 7).

Kinetics similar to that for the formation of ozone was observed in O_2 -containing ClO^- and BrO^- solutions at $pH > 12$. We suggest that ozone is formed by the reaction



in competition with the reaction^{8, 17}



in which XO_m denotes the halogen oxides ClO , BrO and BrO_2 .

Reaction (18) is analogous to the reactions by which O_3^- is oxidized to O_3 by OH and the carbonate radical ion, CO_3^- .^{24, 25}

Ozone was not detected in the photolysis of O_2 -containing alkaline ClO_2^- solutions. In the present experiments this means that the rate constant, k_{18} , for $XO_m = ClO_2$ cannot be greater than *ca.* $10^7 \text{ mol}^{-1} \text{ dm}^3 \text{ s}^{-1}$ and furthermore fits the observation that ClO , which is formed in the primary process (3), reacts fast with the solute, ClO_2^- [reaction (8)].¹⁵

The rate constants, k_{18} , were estimated by assuming that the yield of O_3^- , $Y_{O_3^-}$, is constant during the decay of XO_m . After XO_m had disappeared the solution contained O_3^- and O_3 , the rate of decay of which was small compared with the rate of reaction (18). The yield of O_3^- measured after the decay of XO_m , $Y_{O_3^-}^\infty$, was about half the yield measured initially, $Y_{O_3^-}^0$. With the approximation of a constant value of $Y_{O_3^-}$ the rate equations for reactions (18) and (19) may be integrated and eqn (20) is obtained:

$$(Y_{O_3} - y_{O_3})/Y_{XO_m}^{O_2} = k_{18} Y_{O_3^-} / (2k_{19} Y_{XO_m}^{O_2}) \ln [1 + 2k_{19} Y_{XO_m}^{O_2} / (k_{18} Y_{O_3^-})] \quad (20)$$

This equation relates the ratio of the yield of O_3 formed in reaction (18), $Y_{O_3} - y_{O_3}$, and yield of XO_m , $Y_{XO_m}^{O_2}$, in O_2 -containing solutions with $Y_{XO_m}^{O_2}$ and $Y_{O_3^-}$, which was taken equal to $0.5 \times (Y_{O_3^-}^0 + Y_{O_3^-}^\infty)$. Using values of k_{19} equal to 2.5×10^9 ,⁸ 2.8×10^9 and $7 \times 10^8 \text{ dm}^3 \text{ mol}^{-1} \text{ s}^{-1}$ ¹⁷ for ClO , BrO and BrO_2 , respectively, we find from determination of $Y_{O_3} - y_{O_3}$, $Y_{O_3^-}$ and $Y_{XO_m}^{O_2}$, $k_{18} = 1 \times 10^9$, 1.5×10^9 and $5 \times 10^8 \text{ dm}^3 \text{ mol}^{-1} \text{ s}^{-1}$ for the reaction of O_3^- with ClO , BrO and BrO_2 , respectively.

The yields were calculated from absorbance changes measured at the band maxima of XO_m ,²⁶ O_3^{2-} and O_3 .⁶ For ClO and BrO , $Y_{XO_m}^{O_2} = Y_{XO_m} - Y_{O_3^-}^0$. Y_{XO_m} is the yield of XO_m measured initially in O_2 -free solutions. In accordance with the stoichiometry of reactions (3), (9)–(11) and (19) Y_{XO_m} was calculated from

$$Y_{XO_m} = (\Delta OD_0 - \Delta OD_\infty) / [l(\epsilon_{XO_m} - \frac{1}{2}\epsilon_{XO_m^-} - \frac{1}{2}\epsilon_{XO_{m+1}^-})] \quad (21)$$

where ΔOD_0 is the initial absorbance change and ΔOD_∞ the absorbance change after

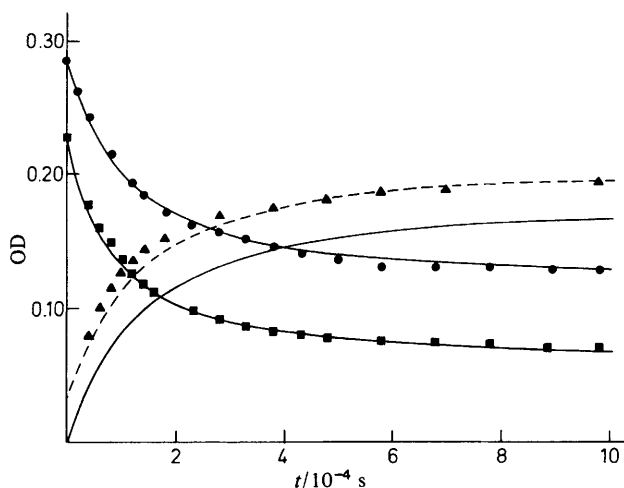


Fig. 8. Absorbance measured at (\blacktriangle) 260 nm, (\bullet) 430 nm and (\blacksquare) 475 nm plotted against time ($t/10^{-4}$ s) after flash irradiation of a solution containing 10^{-3} mol dm^{-3} BrO_3^- , 1.27×10^{-3} mol dm^{-3} O_2 and 0.2 mol dm^{-3} NaOH . Flash light from a conventional flash-photolysis apparatus, flash energy 400 J. Solid curves are computed by numerical integration (see text).

XO_m has decayed. l is the optical length of the cell and $\epsilon_{\text{XO}_m^-}$ and $\epsilon_{\text{XO}_{m+1}^-}$ are the extinction coefficients of the hypohalite ions^{17, 27} and halite ions,^{20, 27} respectively. $Y_{\text{BrO}_2} \text{O}_2$ was calculated from

$$\Delta\text{OD}^{475} = l(\epsilon_{\text{O}_3^-}^{475} [\text{O}_3^-] + \epsilon_{\text{BrO}_2}^{475} [\text{BrO}_2]) \quad (22)$$

$$\Delta\text{OD}^{430} = l(\epsilon_{\text{O}_3^-}^{430} [\text{O}_3^-] + \epsilon_{\text{BrO}_2}^{430} [\text{BrO}_2]). \quad (23)$$

which relate the absorbance changes ΔOD^{475} and ΔOD^{430} to the concentrations (*i.e.* yields) of O_3^- and BrO_2 .

The kinetics of O_3 formation was further studied by conventional flash photolysis of O_2 -saturated solutions containing 10^{-3} mol dm^{-3} KBrO_3 and 0.2 mol dm^{-3} NaOH . Fig. 8 shows the absorbance change measured at 475, 430 and 260 nm plotted against time. Solid curves are calculated from eqn (22) and (23) and from $\Delta\text{OD}^{260} = l\epsilon_{\text{O}_3^-}^{260} [\text{O}_3^-]$. $[\text{BrO}_2]$, $[\text{O}_3^-]$ and $[\text{O}_3]$ are computed by numerical integration of the rate equations for $[\text{BrO}_2]$, $[\text{O}_3^-]$ and $[\text{O}_3]$.

At pH 13.3 $k_{19} = 9.3 \times 10^8$ mol $^{-1}$ dm 3 s $^{-1}$ ¹⁷ was used. k_{18} was determined by the method of trial and error in such a way that the calculated curves for ΔOD^{475} and ΔOD^{430} fitted the experimental points. The curves in fig. 8 were computed with $k_{18} = 7 \times 10^8$ dm 3 mol $^{-1}$ s $^{-1}$. Note that this value agrees fairly well with the value for k_{18} estimated from laser-flash-photolysis measurements ($k_{18} = 5 \times 10^8$ dm 3 mol $^{-1}$ s $^{-1}$). Note also that the difference between the measured and computed values of the absorbance at 260 nm ($\Delta\text{OD}_\infty \approx 0.03$, solid and broken curves in fig. 8) corresponds to $y_{\text{O}_3^-}/y_{\text{BrO}_2} \approx 0.07$, in agreement with the value determined at pH < 10.

Table 1 shows that our measured ratios of $Y_{\text{O}_3}/Y_{\text{XO}_{n-1}}$ are in agreement with those calculated from values of $Y_{\text{O}_3}/Y_{\text{O}^-}$ determined previously.³ In these calculations we have taken $Y_{\text{O}^-} = Y_{\text{O}_3}^\infty$ and $Y_{\text{O}^-} = Y_{\text{XO}_{n-1}} - Y_{\text{O}_3}$.

We thank Prof. A. Weller, Max-Planck Institut für biophysikalische Chemie, Göttingen, and Dr Jerzy Holcman, Risø National Laboratory, for helpful discussions. Financial support from Statens naturvidenskabelige Forskningsråd to U.K.K. is gratefully acknowledged.

- ¹ G. V. Buxton and M. S. Subhani, *J. Chem. Soc., Faraday Trans. 1*, 1972, **68**, 970.
- ² F. Barat, L. Gilles, B. Hickel and B. Lesigne, *J. Phys. Chem.*, 1971, **75**, 2177.
- ³ O. Amichai and A. Treinin, *Chem. Phys. Lett.*, 1969, **3**, 611.
- ⁴ U. K. Kläning and K. Sehested, *J. Chem. Soc., Faraday Trans. 1*, 1978, **74**, 2818.
- ⁵ E. J. Hart, K. Sehested and J. Holcman, *Anal. Chem.*, 1983, **55**, 46.
- ⁶ L. Forni, D. Bahnemann and Edwin J. Hart, *J. Phys. Chem.*, 1982, **86**, 255.
- ⁷ T. Wolff, *J. Photochem.*, 1979, **11**, 215.
- ⁸ U. K. Kläning and T. Wolff, to be published.
- ⁹ E. Bjergbakke, in *Manual of Dosimetry*, ed. N. W. Holm and R. J. Berry (Marcel Dekker, New York, 1970).
- ¹⁰ *Handbuch der präparativen anorganischen Chemie*, ed. G. Brauer (Ferdinand Enke Verlag, Stuttgart, 1962), p. 282.
- ¹¹ G. V. Buxton and M. S. Subhani, *J. Chem. Soc., Faraday Trans. 1*, 1972, **68**, 970.
- ¹² O. Amichai, G. Czapski and A. Treinin, *Isr. J. Chem.*, 1969, **7**, 351.
- ¹³ A. Treinin and M. Yaacobi, *J. Phys. Chem.*, 1964, **68**, 2487.
- ¹⁴ G. V. Buxton and M. S. Subhani, *J. Chem. Soc., Faraday Trans. 1*, 1972, **68**, 947.
- ¹⁵ U. K. Kläning and T. Wolff, to be published.
- ¹⁶ A. Treinin and E. Hayon, *J. Am. Chem. Soc.*, 1975, **97**, 1716.
- ¹⁷ G. V. Buxton and F. S. Dainton, *Proc. R. Soc. London, Ser. A*, 1968, **304**, 427.
- ¹⁸ R. Battino and H. L. Clever, *Chem. Rev.*, 1966, **66**, 39.
- ¹⁹ O. Amichai and A. Treinin, *J. Phys. Chem.*, 1970, **74**, 3670.
- ²⁰ W. H. Koppenol and J. F. Liebman, *J. Phys. Chem.*, 1984, **88**, 99.
D. D. Wagman, W. H. Evans, V. B. Parker, R. J. Schumm, I. Halow, S. M. Bailey, K. L. Churney and R. L. Nattall, *J. Phys. Chem. Ref. Data*, 1982, **11**, supplement no. 2.
- ²¹ *Reactivity of the Hydroxyl Radical in Aqueous Solution*, NSRDS-NBS46 (U.S. Department of Commerce, National Bureau of Standards, Washington D.C., 1973).
- ²² K. Sehested, J. Holcman, E. Bjergbakke and E. J. Hart, *J. Phys. Chem.*, 1982, **86**, 2066.
- ²³ *Selected Specific Rates of Reactions of Transients from Water in Aqueous Solution: Hydrated Electron*, NSRDS-NBS43 (U.S. Department of Commerce, National Bureau of Standards, Washington D.C. 1973 and 1975).
- ²⁴ K. Sehested, J. Holcman, E. Bjergbakke and Edwin J. Hart, *J. Phys. Chem.*, 1984, **88**, 269.
- ²⁵ J. Holcman, K. Sehested, E. Bjergbakke and Edwin J. Hart, *J. Phys. Chem.*, 1982, **86**, 2069.
- ²⁶ *Optical Spectra of Nonmetallic Inorganic Transient Species in Aqueous Solution*, NSRDS-NBS69 (U.S. Department of Commerce, National Bureau of Standards, Washington D.C., 1981).
- ²⁷ T. Chen, *Anal. Chem.*, 1967, **39**, 804.

(PAPER 4/052)